ATLANTIC RESEARCH CORPORATION
HENRY G SHIRLEY MEMORIAL HIGHWAY AT EDSALL ROAD
ALEXANDRIA, VIRGINIA FLEETWOOD 4-3400 TWX ALEX VA. 1089

CHEMISTRY
PHYSICS
ELECTRONICS
ENGINEERING
RESEARCH
DEVELOPMENT
MANUFACTURING
CONSULTING

May 15, 1963

Chief, Bureau of Naval Weapons
Department of the Navy
Washington 25, D. C.

Attention: RMMP-221

Via: Bureau of Naval Weapons Representative
8621 Georgia Avenue
Silver Spring, Maryland

Subject: Transmittal of Quarterly Progress Report
NOrd 15536, Modification 22

Gentlemen:

Enclosed are five (5) copies of the Quarterly Progress Report describing our work in the field of chemical reactions of nozzle materials for solid-propellant rockets for the period February 1 to 30 April 1963. This report has been mailed to the distribution list.

Very truly yours,

ATLANTIC RESEARCH CORPORATION

E. L. Olcott

E. L. Olcott
Director
Materials Division

Enclosure

cc: Direct (1)
ELO:jg

ATLANTIC RESEARCH CORPORATION
ALEXANDRIA, VIRGINIA

CHEMICAL REACTIONS BETWEEN PROPELLANT GASES AND NOZZLE MATERIALS (U)

Third Quarterly Progress Report
Contract NOrd 15536
Modification 22
February 1 to April 30, 1963

Contributors:

R. S. Scheffee
Wm. E. West
J. D. Batchelor
E. L. Olcott

Submitted to:

Bureau of Naval Weapons
Department of the Navy
Washington 25, D. C.

Submitted by:

Atlantic Research Corporation
Shirley Highway at Edsall Road
Alexandria, Virginia

May 15, 1963

LIST OF FIGURES

TABLE OF CONTENTS

ABSTRACT

Hemispherical specimens of AGOT and ZT graphites were exposed to flowing streams of nitrogen, argon, carbon monoxide, and carbon dioxide generated by a plasma torch, and erosion rates were determined. It was found that all gases erode the graphites to a substantial extent with carbon dioxide being especially destructive. It is concluded that chemical reaction and mechanical abrasion (drag) are equally important parameters contributing to the overall erosion rate.

Electrically heated filament specimens (25-mil. diameter) of tantalum carbide (TaC) were exposed to carbon dioxide in the high-pressure bomb and in the vacuum reactor. Losses were determined under a variety of test conditions.

A technique for fabricating niobium carbide (NbC) wires was established, and production of filaments for future reaction studies was started.

Specimens of pyrolytic graphite are being produced in an arc-image furnace by methane decomposition from flowing streams of methane and nitrogen on hemispherical AGOT substrates.

I. INTRODUCTION AND PROCEDURE

This third quarterly progress report for Contract NOrd-15536 (modification 22) describes work done during the period 1 February 1963 through 30 April 1963. The objective of this program is to study the reactions of AGOT graphite, tantalum carbide, and niobium carbide with CO_2, H_2O, HCl and HF. In addition, ZT graphite and pyrolytic graphite are also to be studied. BF_3 is also being considered as a reacting gas. AGOT graphite is a high purity grade graphite of total ash content less than 0.1%. Density of AGOT is 1.7 gms/cc. ZT graphite is a higher density grade, 1.95 gms/cc., but less pure, 0.25% maximum ash content. Pyrolytic graphite approaches theoretical density, 2.2 gms/cc., and is of very high purity.

Erosion rates of the graphites were measured by exposing specimens to the hot gases generated by a plasma torch (Thermal Dynamics Model F-80). The specimens were hemispherical in shape and 0.5-inches in diameter. The plasma torch nozzle was also 0.5-inches in diameter, and specimen-orifice stand-off distances used were 0.25 and 0.5 inches. Seaford-grade nitrogen was used as the primary plasma gas in the torch to extend electrode life; reactive gases were mixed with the hot nitrogen downstream of the electrodes and upstream of the orifice. Erosion rates were established by weighing the specimen before and after exposures of known duration. The effects of temperature rise and decay which occur respectively at the start and finish of exposure are not accounted for, but are only important in short duration (less than 30 sec.) exposures to inert gases.

Reactions of the carbides, TaC and NbC, are being studied at various pressures. The carbide specimens are produced in this laboratory in the form of wires 25 mils in diameter. TaC sample preparation has been described previously*; NbC sample preparation is described elsewhere in this report. The carbide wire test specimens are subsequently used as electrical filaments in an AC circuit and are brought to temperature by direct resistance heating.

---

*1. Atlantic Research Corporation, "Chemical Reactions Between Propellant Gases and Nozzle Materials" (U),Second Quarterly Progress Report, Contract NOrd 15536. Modification 22, February 13, 1963.

The apparatus used for the high pressure tests is shown in Figure 1. The equipment consists essentially of a cylindrical optical bomb, 3 inches ID by 12 inches high and a manifold system. All equipment is stainless steel and designed for operation to 5000 psia. The bomb is fitted with two cylindrical quartz windows, two inches thick, diametrically opposed, providing a 2-inch diameter viewing port from either side of the bomb. The system is purged several times (generally four) at 400 psi before commencing the run. The reacting gas is introduced at the desired pressure, and a voltage is applied to the filament. During the course of the experiment, the temperature is measured and recorded by a two-color pyrometer (Latronics Model CMB3-15214 "Coloratio") and a Varian Associates Model G11A-type A2 recorder. The filament temperature is held constant by adjusting the current through the filament during the test.

The vacuum reaction system is identical in design to that used for carbide test specimen preparation except that a water-cooled cold finger has been added to collect volatile reaction products and the vacuum reactor flask is not water-cooled. As in the case of the high-pressure tests, the filament temperature during a low pressure exposure is kept constant by varying the filament current. Due to the rapid heating and cooling of the filament, the temperature rise and decay times at the start and finish of the exposures are insignificant.

II. EXPERIMENTAL RESULTS

A. The Erosion Rate of AGOT Graphite in Nitrogen and Argon

Hemispherical specimens of AGOT graphite were exposed for 30, 60, 90 and 120 seconds to Seaford-grade nitrogen fed through the plasma torch at feed rates of 150, 250, and 400 SCFH (standard cubic feet per hour). In addition, 60-second exposures to argon at 320 SCFH were carried out. The temperature of the specimens was varied from 2000 to 3000°K. The results of these tests are shown in Figure 2. The curves, which indicate variations of erosion rate with temperature at the selected feed rates, represent weighted averages of the data. In particular, the test curve for nitrogen at 250 SCFH

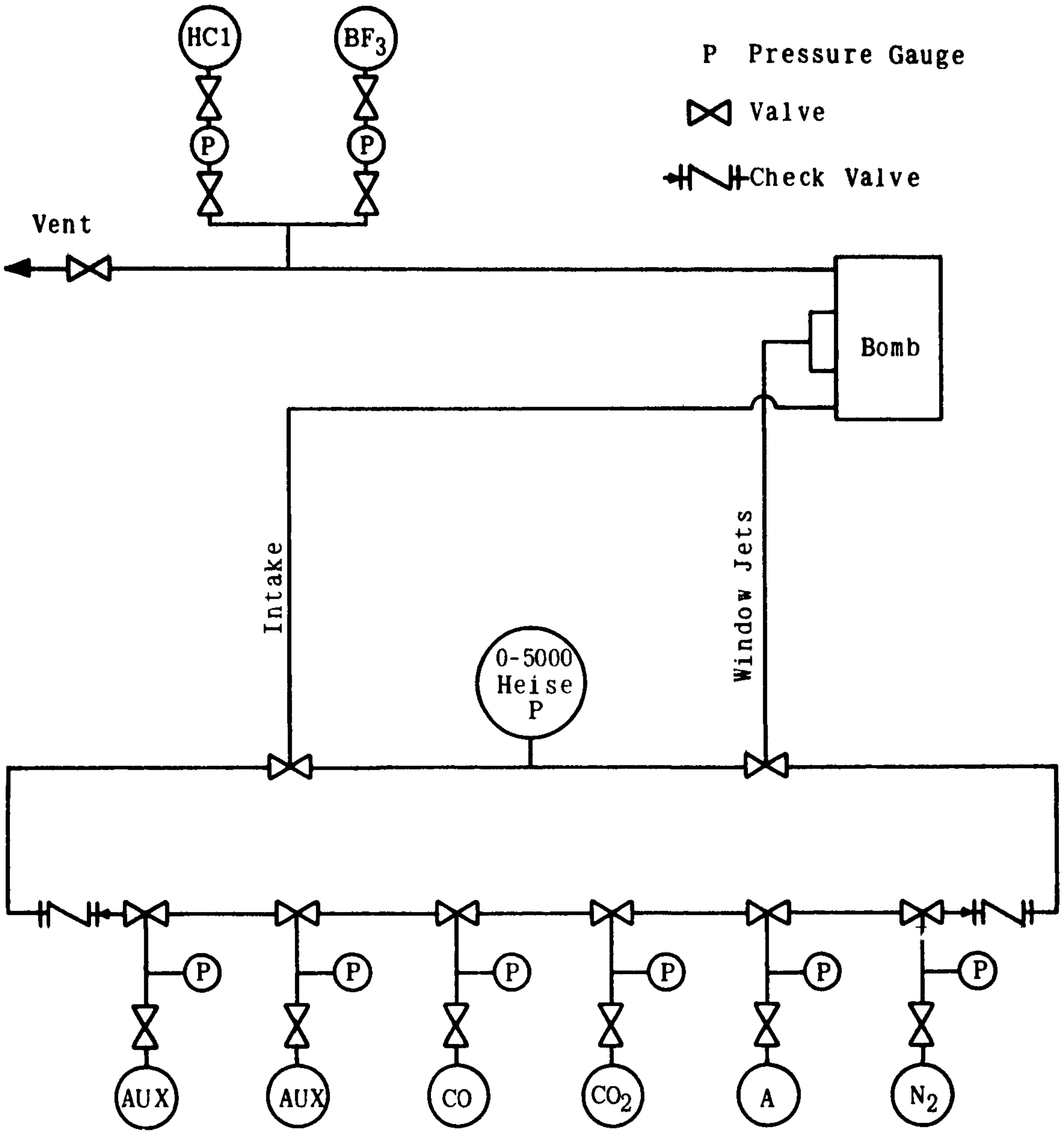

Note:
HCl and BF_3 Intakes are on the Vent Side of the Bomb to Minimize Corrosion to Lines and Gauges in the High-Pressure Side.

29832

Figure 1. High Pressure Experimental Apparatus (schematic).

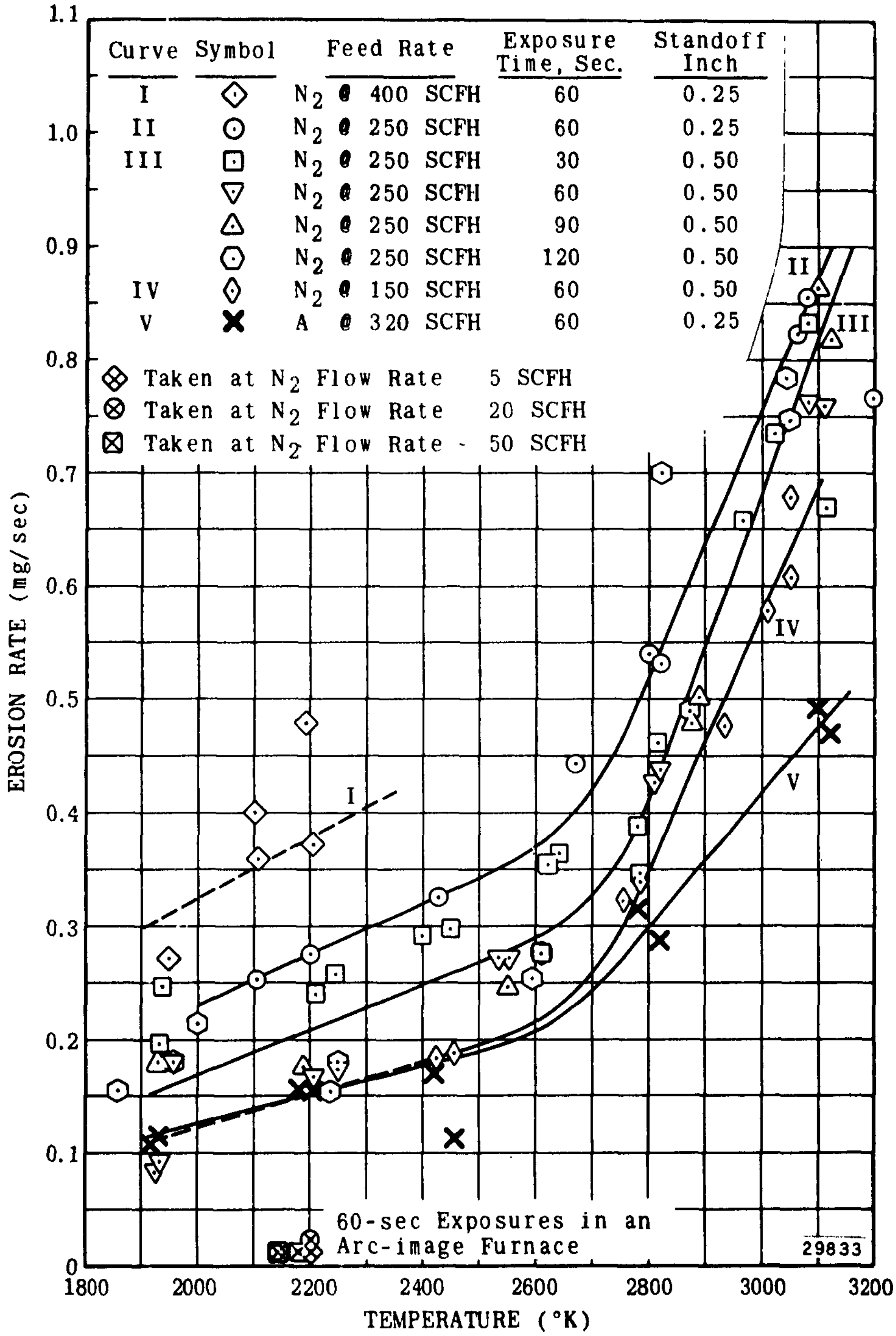

Figure 2. The Erosion Rate of AGOT Graphite in Flowing Streams of Nitrogen and Argon Generated by a Plasma Torch.

is weighted in favor of the long-time exposures in order to minimize the transient effects associated with the 30-second tests.

The data in Figure 2 indicate that erosion rate is a function of temperature and mass flow rate, that erosion in nitrogen is more severe than in argon, and that the rate of change of erosion rate with temperature increases substantially above a transition point at about 2600-2700°K. Curves showing the thermodynamic maximum erosion rates to be expected from either CN(g) or C_3(g) formation are shown in Figure 3. The fact that greater erosion rates were found in nitrogen than in argon despite the higher mass flow rate of the latter, and that the curves in Figure 2 are similar in shape to those for chemical reaction or vaporization, indicate that chemical reactions are at least partly responsible for the measured rates. The weight losses observed in argon and also experiments carried out at low nitrogen feed rates (and velocity) in an arc-image furnace (shown at the bottom of Figure 2) indicate that chemical reactions may not wholly account for the measured erosion rates. Consequently, it must be concluded that erosion is caused by both chemical reaction and mechanical abrasion. Mechanical abrasion appears to predominate at low temperatures (2600°K) and chemical reaction appears to be more important at higher temperatures (2700°K).

To permit an analytical study of the mechanism of loss by mechanical abrasion, calculations were made assuming mechanical losses as a function of drag. Accordingly, we assume

$$R=f(D) \qquad (1)$$

where R=erosion rate, mass/time-area

D=force of drag, per unit area

Defining D as

$$D=\tfrac{1}{2}C_D\rho v^2 \qquad (2)$$

where C_D=drag coefficient

ρ =gas density, mass/volume

v =free stream velocity, length/time.

In addition to the equation for drag, continuity and perfect gases are assumed:

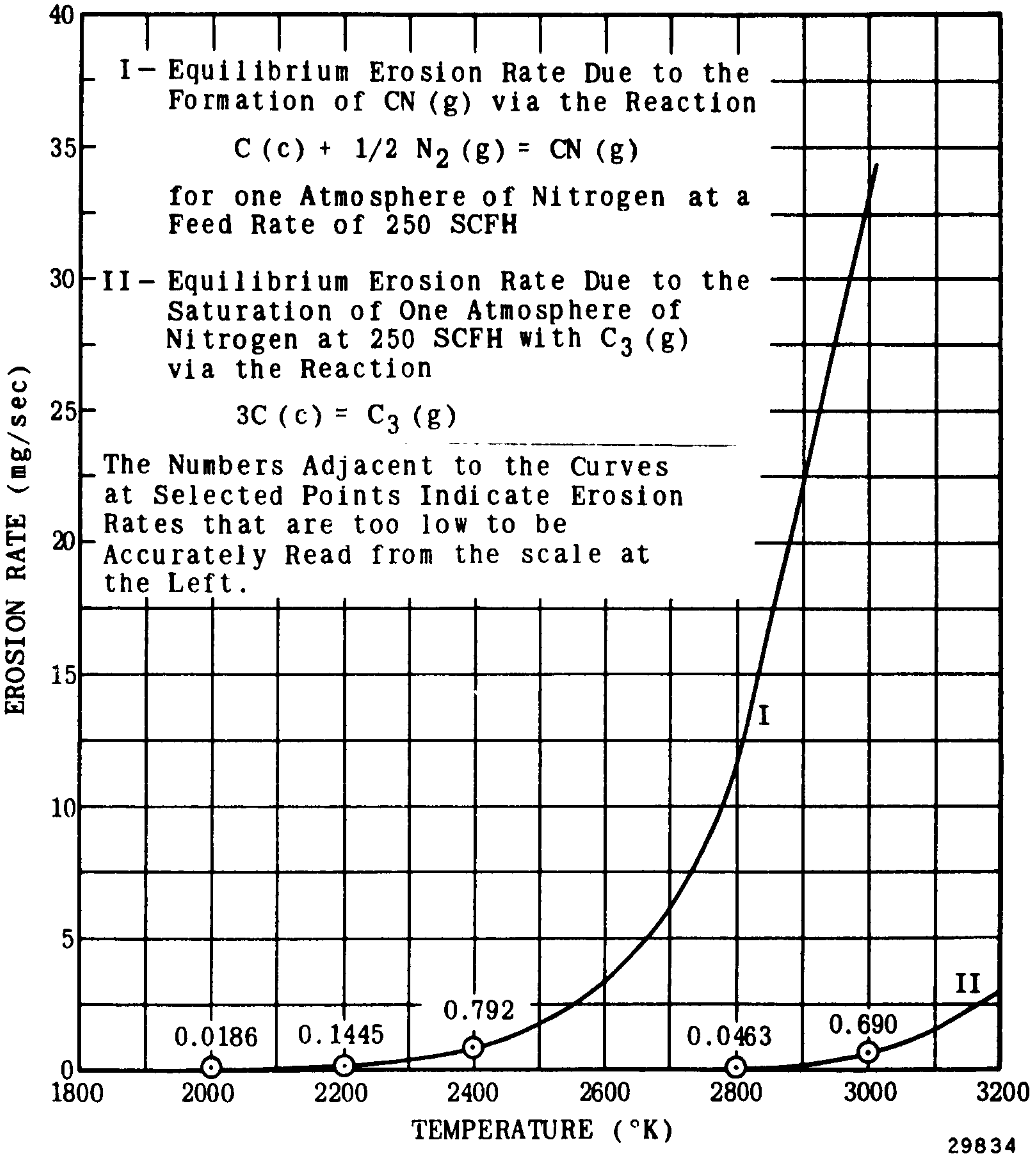

Figure 3. Theoretical Erosion Rate Maximum Due to the Formation of CN(g) or $C_3(g)$.

$$\dot{m} = \rho v A_o \qquad (3)$$

and $$\rho = PM/RT \qquad (4)$$

where $\dot{m}$ = gas feed rate, mass/time

A_o = orifice area

M = gas molecular weight

R = Universal gas constant

T = temperature

Taking the drag coefficient to be inversely proportional to some power of the Reynolds number,

$$C_D \;\alpha\; (Re)^{-n} \;\alpha\; \frac{\mu A_o}{\ell \dot{m}} \qquad (5)$$

where ℓ = characteristic length

Combining equations (1) through (5) yields

$$R = f(K \dot{m}^{2-n} T), \qquad (6)$$

where K is assumed constant and contains all terms except $\dot{m}$ and T.

From the appearance of the curves in Figure 2, the low temperature data seem to obey equation (6) in that erosion rate is a linear function of temperature and $(\partial R/\partial T)_{\dot{m}}$ is a function of mass flow rate. In view of this, the following correlation equations were found which represent the data for the exposures to nitrogen at temperatures below 2600°K:

$$\dot{m}_{c,.5} = 1.25 \times 10^{-4}\, T\, (\dot{N}_2)^{0.6} - 0.24 \quad (T < 2600°K) \qquad (7a)$$

$$\dot{m}_{c,.25} = 1.365 \times 10^{-4}\, T\, (\dot{N}_2)^{0.6} - 0.22 \quad (T < 2600°K) \qquad (7b)$$

where,

$\dot{m}_{c,.5}$ = erosion rate at 0.5-inch specimen standoff from orifice, mg/sec.

$\dot{m}_{c,.25}$ = erosion rate at 0.25-inch specimen standoff from orifice, mg/sec.

T = temperature, °K

$\dot{N}_2$ = mass flow rate of nitrogen, gm/sec.

$$\dot{m}_{c,.5} = 571\ \dot{N}_2^{\,0.32} \exp(-2.1\mathrm{x}10^4/T) \qquad (T > 2700°K) \qquad (8a)$$

$$\dot{m}_{c,.25} = \dot{N}_2^{\,0.32} \exp(-1.54\mathrm{x}10^4/T) \qquad (T > 2700°K) \qquad (8b)$$

Equations 7 and 8 do not prove that erosion is caused by abrasion at the low temperatures and by chemical reaction/vaporization at the high temperatures. Quite obviously, a modest amount of chemical reaction occurs at temperatures less than 2600°K during nitrogen exposures, since greater erosion rates were found for these exposures than for argon exposures despite the higher mass flow rate of the latter. Further, a modest amount of vaporization is probably responsible for the increase in slope of the erosion rate-temperature curve for nitrogen exposures above 2600°K. It can only be concluded from the data that erosion is caused by abrasion, chemical reaction, and vaporization and that these phenomena are interdependent in a complex manner. The relative importance of these different phenomena at various flow rates and temperatures can only be ascertained qualitatively from these experiments. More quantitative definition of the phenomena would require experiments considerably more sophisticated than those employed. Here, abrasion has been assumed to be a function of drag (equation 1), chemical reaction effects have been assumed to be an exponential function of temperature (Arrehnius model) and these assumptions have been used simply as foundations for expressing the data. Taken in this light, equations (7) and (8) reflect qualitatively the relative importance of mechanical and chemical effects, and thus represent convenient semi-empirical, engineering correlations of the data. In particular, the temperature coefficients of log $\dot{m}$ in equations (8) should not be interpreted as activation energies, since abrasion effects were necessarily included in their deviation.

B. The Erosion Rate of AGOT Graphite in Carbon Dioxide

Hemispherical specimens, 0.5 inch in diameter, of AGOT graphite were exposed for 30 and 60-second durations to mixtures of nitrogen, carbon monoxide, and carbon dioxide. These experiments were carried out in the plasma torch at orifice-specimen standoff distances of 0.5 and 0.25 inches. The experimental procedure consisted of preheating the specimen for 30 seconds in nitrogen, after which carbon monoxide, carbon dioxide or both were introduced at known feed rates for 30 or 60 seconds. The nitrogen was used as the carrier gas in the torch, with CO and CO_2 being introduced at room temperature downstream of the electrodes in a mixing chamber placed upstream of the final orifice. The chamber was designed to produce a large scale of turbulence in order to ensure complete mixing and heat transfer between the gases. The nitrogen feed rate was held constant at 250 SCFH throughout the experiments. Carbon dioxide was added at rates of 50 and 100 SCFH, and carbon monoxide was added at a rate of 50 SCFH. The experimental data are given in figures 4 and 5.

Figure 4 shows the weight loss suffered by the specimens as a function of temperature for 30 and 60 second exposures to CO_2 at feed rates of 50 and 100 SCFH. The data indicate that the weight loss is a function of temperature, time of exposure, and CO_2 feed rate, all anticipated effects. The data in Figure 4 were converted to erosion rates and corrected for the effect of nitrogen by applications of equations (7a) and (8a). It was found that the erosion rate is an exponential function of temperature and a power function of CO_2 feed rate. The data reduced nicely to the following:

$$\dot{m}_{c,\,CO_2} = 50.5\ (\overline{\dot{CO}_2})\ 0.683\ \ \exp\ (-4850/T)\ + \dot{m}_{c,.5} \qquad (9)$$

where

$\dot{m}_{c,CO_2}$ = erosion rate of AGOT graphite due to CO_2, mg/sec.

$\overline{\dot{CO}_2}$ = mass flow rate of CO_2, gm/sec.

$\dot{m}_{c,.5}$ = erosion rate of AGOT graphite due to N_2, expressed by either equation (7a) or (8a) depending on temperature, mg/sec.

Although equation (9) correlates the data well, it must be realized that the effects of both abrasion and chemical reaction are included and are interrelated. It should be noted that the temperature dependency is much less than would be expected for chemical reaction controlling (the activation energy is about 40 Kcal for gasification by CO_2) but much steeper than for

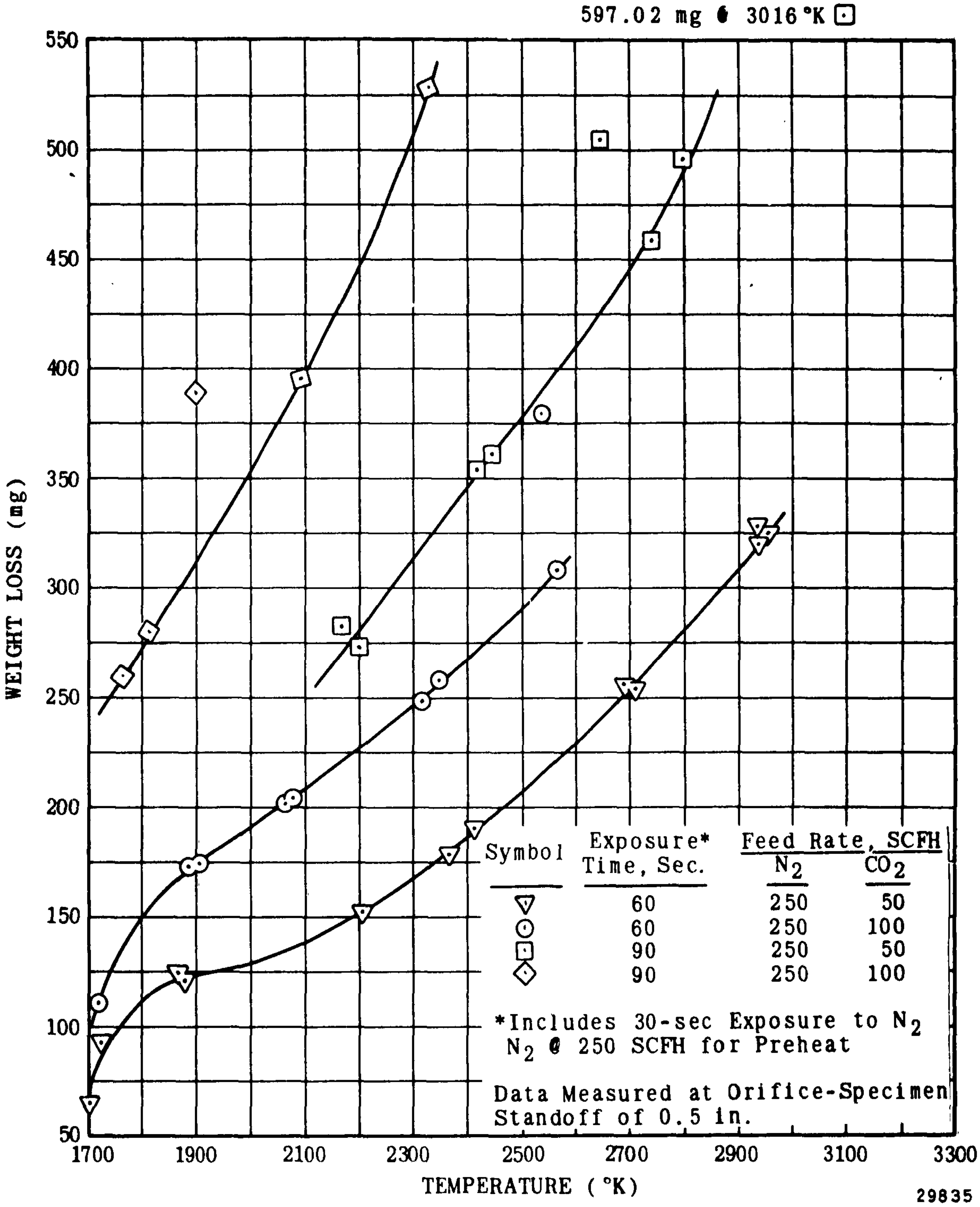

Figure 4. Effect of Temperature and Gas Composition on the Weight Loss of AGOT Graphite in Flowing Streams of Nitrogen and Carbon Dioxide.

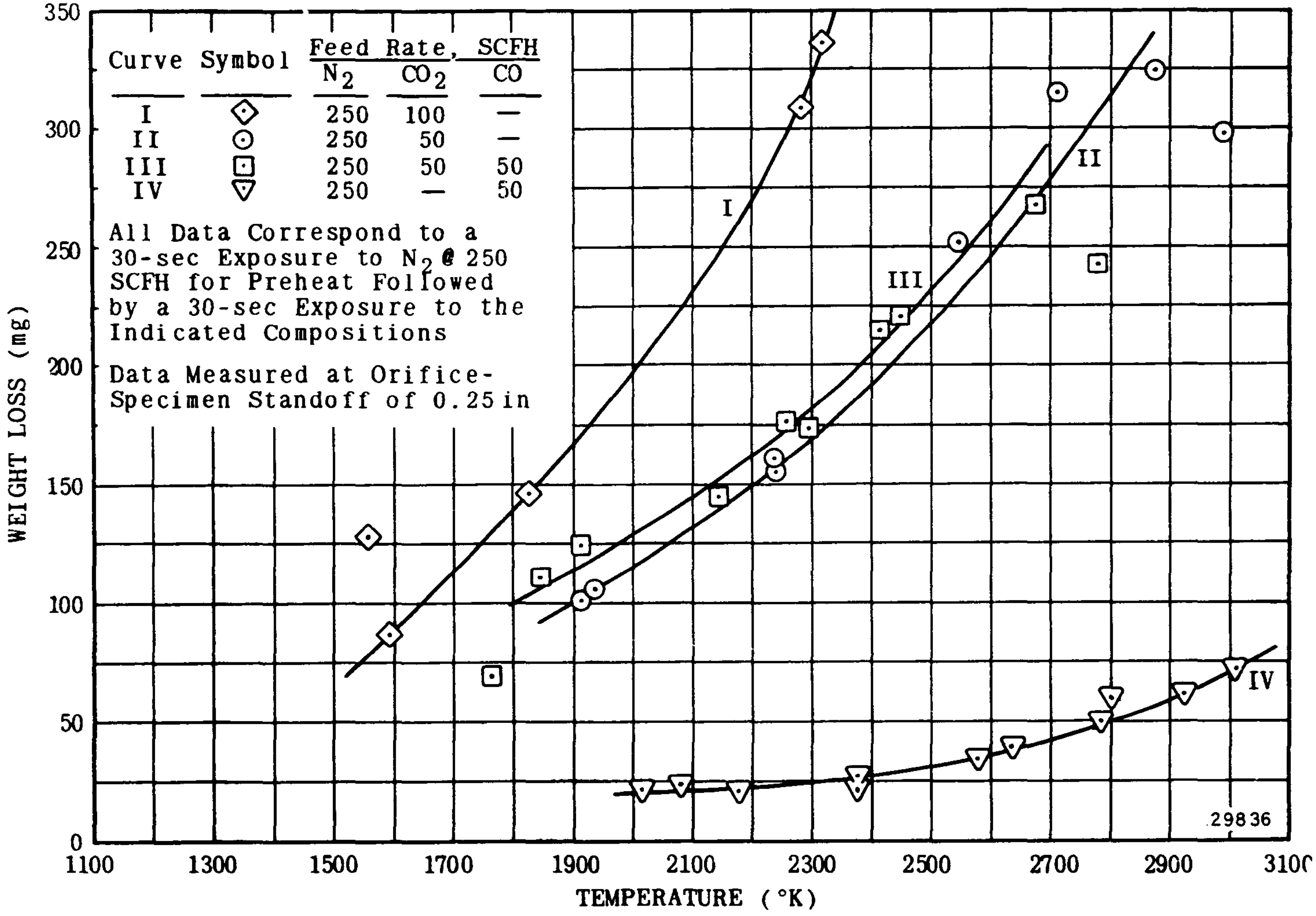

Figure 5. Effect of Temperature and Gas Composition on the Weight Loss of AGOT Graphite in Flowing Streams of Nitrogen, Carbon Monoxide, and Carbon Dioxide.

diffusion control since the temperature exponent is of the order of 2 rather than the anticipated 0.5 for a diffusion process. Undoubtedly, abrasion is the contributing factor in the difference between the temperature dependency found here and that found in more classical kinetic experiments. As noted previously, the interrelationship between abrasion and chemical reaction is a complex one and can, at best, only be defined qualitatively. Nevertheless, equation (9) reflects the importance of chemical reaction to the erosion rate of AGOT graphite in CO_2.

The data in Figure 5 largely parallel those in Figure 4 for the pure CO_2 runs providing a correction term is used for the influence of standoff distance. This is apparently a stagnation effect.* The interesting phenomenon to be seen in Figure 5 is the surprisingly high weight losses found for the experiments with carbon monoxide. In the CO-N_2 experiments (curve IV) the weight losses are significantly greater than those predicated by equations (7b) or (8b), indicating that CO may be reacting with the specimen. Although reaction is meaningless from a thermodynamic standpoint, some process of importance to the kinetics of erosion does occur. It is suggested that a carbon exchange may be taking place. If excited CO molecules are absorbed on the AGOT surface, the original (CO) bond is broken, and the C atom is carried away, then the remaining oxygen atom may react with the C site to form CO which is subsequently desorbed. This is only postulation, of course, but something of a chemical nature is apparently taking place since CO is quite obviously not as inert to AGOT graphite as is N_2. The experiments with CO-CO_2-N_2 mixtures (curve III) yielded higher erosion rates than those with CO_2-N_2 mixtures (curve II). Carbon monoxide should contribute to the erosion rate of AGOT by abrasion (mass velocity) effects and by the apparent chemical reactivity noted above, but should inhibit the CO_2 reaction by competing for adsorption sites. The differences between the curves II and III can be accounted for approximately by equation (7b), indicating the higher erosion rates found for N_2-CO-CO_2 mixtures are due to increased abrasion. Apparently, the contribution to erosion rate by CO reactivity is roughly off-set by the inhibition of the reaction with CO_2.

---

*Actually, this effect cannot be explained from incompressible flow equations since the velocity profiles at 0.25 and 0.5 inch standoff distances would not be significantly different for the gas velocities employed in these experiments. Theoretical compressible flow equations were not considered because the effort did not appear justified.

C. The Erosion Rate of ZT Graphite in Nitrogen and Carbon Dioxide

A limited number of experiments were carried out with ZT graphite using the plasma torch. Hemispherical specimens, 0.6 inch in diameter, were used in the tests, and the orifice-specimen standoff distance was 0.25 inch. One series of tests was run at 250 SCFH of N_2, 60-second exposures. A second series was conducted with CO_2, utilizing a 30-second preheat time with 250 SCFH of N_2 followed by a 30-second exposure to 50 SCFH of CO_2 plus 250 SCFH of N_2. The results of these experiments are given in Figure 6.

In comparison with AGOT, ZT graphite erodes faster in pure N_2 but not as fast in CO_2, particularly at the higher temperatures. In contrast to AGOT, the erosion of ZT in N_2 is linear with temperature throughout the entire temperature range, indicating that this material is more susceptible to abrasive erosion but less affected by chemical attack than is AGOT. Although the erosion of ZT in N_2 is linear with temperature, the slope ($\partial \dot{m}_c/\partial T$) is steeper than that for AGOT, the curves not being parallel at any temperature. Conversely, the temperature dependence of the erosion rate of ZT in CO_2 is flatter than that for AGOT. In addition, the CO_2 erosion data for ZT seems to fit better when expressed as a power function of temperature (approximately, $\log \dot{m}_c \propto 4.25 \log T$) than as an exponential function of temperature. No further data correlation was carried out due to the limited number of experiments planned on this material. Rather, the analysis was restricted to the comparisons with AGOT described above.

D. Studies of Tantalum Carbide Reactions

1. Low Pressure Experiments

To date, a total of 37 wire specimens of tantalum carbide (TaC) 25 mils in diameter have been studied at various temperatures and reactant gas compositions in low-pressure (less than one atmosphere absolute) experiments. Gas compositions used included mixtures of CO, CO_2, H_2, H_2O and argon. The results of these experiments are tabulated in Table 1.

In these experiments a TaC wire, 25 mils in diameter by approximately two inches in length, was connected to two electrodes enclosed in a two-liter Pyrex reactor. The wire specimen was an integral part of an electric circuit and was brought to the desired temperature by resistance heating. The reactor

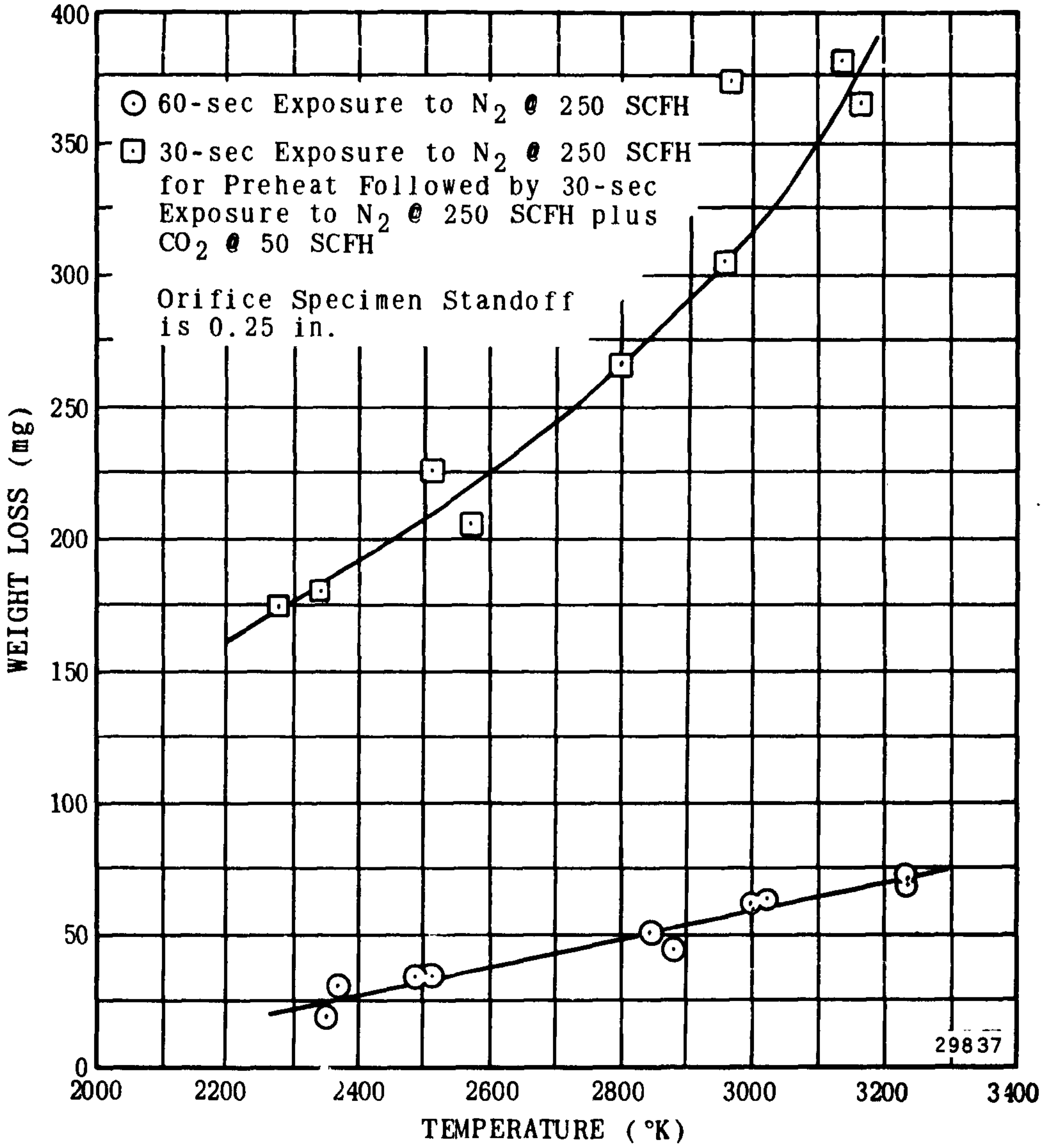

Figure 6. Effect of Temperature and Gas Composition on the Weight Loss of ZT Graphite in Flowing Streams of Nitrogen and Carbon Dioxide.

was evacuated to 5 to 10 μHg, charged to the selected pressure with reactant gases of the desired composition, and the filament (TaC wire) was brought quickly to temperature for reaction. The temperature of the wire at its mid-point was recorded and held constant throughout the run. Weight changes of the specimens were determined by weighings before and after the reaction.

Due to the quiescent nature of the experimental condition, the weight changes reported here are due only to chemical reaction effects, and not to any mechanical abrasion as found in plasma torch experiments. To aid in interpreting the experimental results, it is well to keep in mind that TaC reacts with either CO_2 or H_2O to form Ta_2O_5 or other oxides and that the melting point of Ta_2O_5 (c) is 2150°K. Ta_2O_5 vaporizes incongruently to a modest extent in the temperature range 2000-3000°K forming TaO (g) and TaO_2 (g). Further, it should be noted that the mid-point temperature of the filament is the highest on the surface of the filament; the temperature drops several hundred degrees in the vicinity of the electrodes.

a. TaC-CO_2-Argon Experiments (Tests TaC-2 through TaC-12)

The results of tests carried out on TaC filaments in CO_2-Argon gas mixtures are shown in Runs TaC-2 to TaC-12 in Table 1. Filament burnout, caused by complete oxidation through the filament crossection was experienced only in the 3000°K tests. In these tests, the Ta_2O_5 (l) film formed by reaction was quite fluid and coalesced to beads on the filament. As the beads coalesced they moved along the filament by surface tension effects and as the bead passed through the line-of-sight of the optical pyrometer, the temperature fell due to the lower temperature of the outside of the oxide bead caused by radiation losses. Due to the fluid nature of Ta_2O_5 (l) at 3000°K, causing coalescence, the Ta_2O_5 (l) did not form a good barrier to diffusion, and burnout of the filament occurred rather quickly. At lower temperatures (2500°K and below), the Ta_2O_5 (l) film was not so fluid, remained relatively stationary, and constituted a sufficient barrier to CO_2 diffusion to prevent filament burnout. Of course, at 1920°K, Ta_2O_5 (c) was formed and also prevented burnout. It is evident from the data that TaC is severely affected by CO_2. It is also probable that due to the fluid nature of Ta_2O_5 (l) and the flaky (i.e.rough) nature of the Ta_2O_5 (c) coatings formed during reaction, TaC would be even more severely attacked by high velocity flows of CO_2 since the oxide coatings would very likely be scrubbed away.

TABLE I

Tantalum Carbide (TaC) Filament Tests in $CO-CO_2$ and H_2-H_2O Gas Mixtures

Test No.	Gas	Initial Partial Pressure (mm Hg)	Temperature °K	Reaction Time (sec.)	Filament Weight, mg. Initial	Final	Change	Observations (Note: c.f. is abbreviation for cold finger)
TaC-2	A	400	3035	60	339.13	339.02	-0.11	Filament turned to silver in color. No deposit on c.f.
TaC-3	CO_2	66	3035		338.92	320.65	-18.27	Burn out: seven shiny beads at regular intervals along the filament presumably Ta_2O_5. Blue-white deposit on c.f.
TaC-4	A CO_2	475 66	3035	19	337.76	331.05	-6.71	Burn out; observations similar to TaC-3
TaC-5	A CO_2	475 66	2480	60	336.47	338.41	+1.94	No burn out; no deposit on c.f., three beads on filament; rough surface coating, "gun-metal gray" in color, presumably Ta_2O_5 crystals
TaC-6	A CO_2	475 66	2480	62	340.05	342.43	+2.38	No burn out; observations similar to TaC-5
TaC-7	CO_2	66	2480	60	338.46	315.71	-22.75	Filament spits small particles during test run which fused to the reactor vessel walls; no beads on filament; rough gray coating on filament; tan-colored deposit on c.f.
TaC-8	A CO_2	475 66	1920	60	337.85	338.66	+0.81	Dark gray crystalline coating on filament. No deposit on c.f.
TaC-9	CO_2	66	1920	60	337.90	338.83	+0.93	Same as TaC-8
TaC-10	CO_2	66	1920	60	337.14	337.94	+0.80	Same as TaC-8
TaC-11	A CO_2	475 66	3035	23	335.86	331.25	-4.61	Burn out; part of filament fell to bottom of reactor and fused to reactor walls; bead formation on filament; pale blue-white deposit on c.f.
TaC-12	A CO_2	475 66	2535	60	337.22	336.58	-0.62	No burn out; three beads on filament; gray crystalline coating on filament; no deposit on c.f.
TaC-13	A CO CO_2	409 66 66	2420	60	335.91	337.73	+1.82	Same as TaC-12
TaC-14	A CO CO_2	409 66 66	2420	60	336.73	336.00	-0.73	Same as TaC-13
TaC-15	CO CO_2	66 66	2420	60	338.11	308.30	-29.8	Gray deposit on c.f.; gray crystalline coating on filament bead formation on filament
TaC-16	A CO CO_2	409 66 66	1920	60	336.86	337.50	+0.64	No deposit on c.f.; gray crystalline coating on filament; no bead formation

TABLE I (Cont'd)

Tantalum Carbide (TaC) Filament Tests in $CO-CO_2$ and H_2-H_2O Gas Mixtures

Test No.	Gas	Initial Partial Pressure (mm Hg)	Temperature °K	Reaction Time (sec.)	Filament Weight, mg.			Observations (Note: c.f. is abbreviation for cold finger)
					Initial	Final	Change	
TaC-17	A CO CO_2	409 66 66	1920	60	337.38	338.10	+0.72	Same as TaC-16
TaC-18	CO CO_2	66 66	1920	60	335.67	336.20	+0.53	Same as TaC-16
TaC-19	CO	60	2920	60	337.74	337.80	+0.06	Filament changed color to a dull silver: no deposit on c f
TaC-20	A H_2O	90 67.1	1920	54	336.17	344.61	+8.44	Burn out; filament was not broken but was oxidized throughout; large flaky gray coating on filament; no deposit on c.f.
TaC-21	A H_2O	89 59	1920	60	338.44	346.10	+7.66	Same as TaC-20
TaC-22	A H_2O	121 77	2370	28	264.95	273.2	+8.15	Same as TaC-20
TaC-23	A H_2O	137 40	2410	54	332.26	292.80	-39.46	Burn out; shiny black beads along filament; filament coated with shiny black glossy coating; no deposit on c.f.
TaC-24	A H_2O	30 20	1920	50.5	337.51	346.54	+9.03	Burn out; uniform gray coating on filament; no deposit on c.f.
TaC-25	A H_2O	30 20	1920	60	337.41	348.01	+10.60	Same as TaC-24
TaC-26	A H_2O	30 20	2540	71	336.50	267.80	-68.7	Filament spits particles during test run; black coating on filament; gray deposit found on walls of reactor
TaC-27	A H_2O	42 20	2540	58.5	336.84	248.00	-88.84	Burn out; black coating on filament; gray deposit on walls of reactor
TaC-28	A H_2O	34 20	2540	60	332.09	267.50	-64.59	Same as TaC-27 except no burn out
TaC-29	A H_2O	33 20	3035	12.6	331.08	293.6	-37.5	Burn out; smooth shiny black coating on filament; light blue deposit on reactor walls
TaC-30	A H_2O	40 20	3035	47	340.62	264.90	-75.72	Same as TaC-29 except filament coating was not as smooth; bead formation

TABLE I (Cont'd)

Tantalum Carbide (TaC) Filament Tests in CO-CO_2 and H_2-H_2O Gas Mixtures

Test No.	Gas	Initial Partial Pressure (mm Hg)	Temperature °K	Reaction Time (sec.)	Filament Weight, mg. Initial	Final	Change	Observations (Note: c.f is abbreviation for cold finger)
TaC-17	A CO CO_2	409 66 66	1920	60	337.38	338.10	+0.72	Same as TaC-16
TaC-18	CO CO_2	66 66	1920	60	335.67	336.20	+0.53	Same as TaC-16
TaC-19	CO	60	2920	60	337.74	337.80	+0.06	Filament changed color to a dull silver: no deposit on c f
TaC-20	A H_2O	90 67.1	1920	54	336.17	344.61	+8.44	Burn out; filament was not broken but was oxidized throughout; large flaky gray coating on filament; no deposit on c.f.
TaC-21	A H_2O	89 59	1920	60	338.44	346.10	+7.66	Same as TaC-20
TaC-22	A H_2O	121 77	2370	28	264.95	273.2	+8.15	Same as TaC-20
TaC-23	A H_2O	137 40	2410	54	332.26	292.80	-39.46	Burn out; shiny black beads along filament; filament coated with shiny black glossy coating; no deposit on c.f.
TaC-24	A H_2O	30 20	1920	50.5	337.51	346.54	+9.03	Burn out; uniform gray coating on filament; no deposit on c.f.
TaC-25	A H_2O	30 20	1920	60	337.41	348.01	+10.60	Same as TaC-24
TaC-26	A H_2O	30 20	2540	71	336.50	267.80	-68.7	Filament spits particles during test run; black coating on filament; gray deposit found on walls of reactor
TaC-27	A H_2O	42 20	2540	58.5	336.84	248.00	-88.84	Burn out; black coating on filament; gray deposit on walls of reactor
TaC-28	A H_2O	34 20	2540	60	332.09	267.50	-64.59	Same as TaC-27 except no burn out
TaC-29	A H_2O	33 20	3035	12.6	331.08	293.6	-37.5	Burn out; smooth shiny black coating on filament; light blue deposit on reactor walls
TaC-30	A H_2O	40 20	3035	47	340.62	264.90	-75.72	Same as TaC-29 except filament coating was not as smooth; bead formation

TABLE I (Cont'd)

Tantalum Carbide (TaC) Filament Tests in CO-CO_2 and H_2-H_2O Gas Mixtures

Test No.	Gas	Initial Partial Pressure (mm Hg)	Temperature °K	Reaction Time (sec.)	Filament Weight, mg. Initial	Final	Change	Observations (Note: c.f. is abbreviation for cold finger)
TaC-31	A H_2O	30 20	3035	10	338.21	318.90	-19.31	Same as TaC-30
TaC-32	A H_2O	33 20	3035	8	333.29	319.0	-14.29	Same as TaC-31
TaC-33	A H_2 H_2O	26.7 3.3 20	1920	60	336.17	348.20	+12.03	Gray coating on filament; no deposit on c.f.
TaC-34	A H_2 H_2O	30.8 3.3 20	1920	60	335.75	344.3	+8.55	Same as TaC-33
TaC-35	A H_2 H_2O	30.8 3.3 20	2540	60	331.85	257.0	-74.85	Black coating on filament; gray deposit on walls of reactor
TaC-36	A H_2 H_2O	26.7 3.3 20	2540	60	329.23	249.5	-79.73	Same as TaC-35
TaC-37	A H_2 H_2O	26.7 3.3 20	3035	15	331.69	293.8	-37.89	Burn out; filament covered with shiny black beads; light blue deposit on reactor walls

b. TaC-CO_2-CO-Argon Experiments (Tests TaC-13 through TaC-18)

The presence of CO has no inhibiting effect on the attack of TaC by CO_2. The behavior of TaC in CO_2-CO-Argon mixtures was not essentially different from the behavior of TaC in CO_2-Argon mixtures.

c. TaC-H_2O-Argon Experiments (Tests TaC-19 through TaC-32)

The data indicate that TaC is severely attacked by H_2O, to a greater extent than the attack by CO_2. Not only are burnout times shorter in H_2O, but the weight changes are also greater. This indicates that the reaction mechanism between TaC and H_2O is very probably much different to that between TaC and CO_2. In particular, it seems that metastable intermediates (probably hydroxides) are formed in the H_2O reactions, which permit reaction to proceed relatively unhindered (explaining the low temperature burnouts) and relatively fast (explaining the large weight losses during the short-time high-temperature tests).

d. TaC-H_2-H_2O-Argon Experiments (Tests TaC-33 through TaC-37)

In similarity to the influence of CO on CO_2 attack, H_2 has no inhibiting effect on the attack of TaC by H_2O.

It is concluded from the low pressure measurements described above that TaC is not a suitable rocket nozzle material for motors which use propellants yielding large amounts of CO_2 or H_2O. Quite obviously TaC is far too reactive with H_2O or CO_2 for such use. In nozzle service the abrasive effects of the high velocity gas stream would most likely scrub away the oxide film as fast as it formed, thus preventing any protection of the TaC by the oxide acting as a diffusion barrier.

The high pressure test results in Table II show the strong attack of carbon dioxide on TaC. Above 2150°K the oxide is molten. In most cases the oxide flowed to the bottom of TaC wire exposing additional carbide surface to CO_2. In pure CO_2 above 2300°K the burnout time varied from 3 to 10 seconds. The burnout time depended mostly on the nature of the oxide flow rather than the temperature and pressure conditions. In rocket nozzle applications the oxide would again provide even less protection than in these tests.

E. Preparation of Niobium Carbide Test Specimens

A reproducible method of producing niobium carbide wires was developed. The C/Nb mole ratio (measured by weight gain) is 0.77 to 0.81.

TABLE II

High Pressure Tests of TaC Wires in CO_2 and CO_2-A Mixtures

Test No.	Gas	Initial Partial Pressure psi.	Mean Temperature °K	Reaction Time (sec.)	Filament Weight, mg.		Filament Length, inc.		Remarks
					Initial	Change	Total	Reacted	
T-2	CO_2	165	1890	45					Burn out. Wire diameter increases 50 to 100% by white crystalline oxide growth
T-3	CO_2	175	1980	45			1.38	0.80	Same as T-2
T-5	CO_2	165	2250	15	144.9	+8.4	1.12	0.80	Burn out; bead of molten black oxide on wire
T-7	CO_2	165	2350	9	210.8	+5.6	1.65	0.90	Burn out; molten oxide appeared to bubble during test. Small loss of oxide observed
T-8	CO_2	135	1800	25.5	210.9	+9.5	1.62	0.84	Same as T-2
T-9	CO_2	15	1830	80	222.0	+2.8	1.72	0.50	Burn out; same as the oxide flaked off wire
T-10	CO_2	215	2700	10	191.0	-22.8	1.47	0.92	Burn out. 4 small beads of black oxide
T-11	CO_2	15	2700	4	203.6	-17.6	1.56	0.96	Same as T-10
T-12	CO_2	90	2370	31.4	142.0	+9.6	1.10	0.87	Burn out. 5 reflective oxide beads on wire
T-13	CO_2	15	2400	38	208.2	+7.0	1.61	0.66	Burn out. Oxide coating on wire. Less flow of oxide than previous tests.
T-14	CO_2 A	15 380	2250	260	191.4	+14.4	1.47	1.22	Burn out. 5 large oxide beads on wire
T-15	CO_2	15	3000	28.2	188.0	-1.6	1.44	0.72	4 small beads on wire, dark gold in color. Burn out.
T-17	A	150			164.2	+2.9			
T-18	CO_2	50	2450	12	195.3	+2.0	1.50	0.96	Burn out; one large bead of oxide hanging from middle of wire
T-19	CO_2 A	50 50	2500	22	207.2	+2.9	1.58	0.92	Burn out; four large reflective beads hanging from wire
T-20	CO_2	100	2460	11.5	224.6	+2.4	1.72	0.97	Burn out; three large beads hanging from wire

TABLE II (Cont'd)

High Pressure Tests of TaC Wires in CO_2 and CO_2-A Mixtures

Test No.	Gas	Initial Partial Pressure psi	Mean Temperature °K	Reaction Time (sec.)	Filament Weight, mg.		Filament Length, inc.		Remarks
					Initial	Change	Total	Reacted	
T-21	CO_2	50	2450	39	168.1	+4.0	1.28	0.95	Burn out; 3 large reflective beads hanging from wire
	A	150							
T-22	CO_2	50	2920	3	164.3	-7.0	1.26	1.02	Burn out; 5 small black beads hanging from wire
	A	150							
T-23	CO_2	165	2500	9	204.2	+2.5	1.58	1.00	Burn out; 3 long black beads hanging from wire

The wire is silver colored with a bright metallic luster. It is brittle but has adequate strength for handling and mounting.

Storms and Krikorian* present a phase diagram for C/Nb which shows formation of two carbides, Nb_2C and NbC. Niobium melts at 4400°F. Niobium and Nb_2C form a eutectic melting at 4230° ± 40°F. From compositions of $NbC_{0.39}$ to $NbC_{0.52}$ the melting point increases rapidly to a peritectic temperature of 5600 ± 140°F at $NbC_{0.86}$. The melting point of the wires used in the study (C/Nb ratio = 0.77 to 0.81) should be 100 to 200°F below the maximum. A niobium carbide wire heated in 14 atm of carbon monoxide in the optical bomb melted at 6080°F. The wire was tarnished and had a weight loss of 5 percent. The melting temperature was measured with a Latronics Corp. two-color pyrometer. This test result is in substantial agreement with the phase diagram of Storms and Krikorian.

The procedure and equipment for preparing test pieces of niobium carbide wires is similar to that used to produce tantalum carbide. A 25-mil niobium wire is heated at temperatures from 4200 to 5000°F in a hydrogen-ethylene atmosphere at somewhat below atmospheric pressure. There is only a trace of carbon deposition at the mounting posts. The C/Nb ratio can be varied by changing the wire temperature. Wires have been produced with C/Nb mole ratios above 0.9. Higher ratios can probably be obtained but may not be desirable due to the reduced melting point.

A 2-1/2 inch length of 25-mil diameter niobium wire is mounted between brass electrodes in a 2-liter vacuum flask (the total capacity of flask with head is about 2.6 liters). The flask is connected to the gas and vacuum manifold and immersed in a water bath that is kept below 50°F. The electrodes are connected to a variable voltage source. The container is evacuated to less than one mm. of Hg abs (usually 10^{-1} to 10^{-2} mm), filled with hydrogen, and evacuated a second time. Ethylene is added to 10 mm. of Hg abs. Hydrogen is added to provide a total pressure of 500 ± 20 mm of Hg abs. During the run the total pressure approaches one atmosphere.

---

*Storms, E. R. and N. H. Krikorian, "The Niobium-Niobium Carbide System," J. Phys. Chem., Vol. 64 (October 1960), pp. 1471-77.

Voltage is applied to the wire until a current of 38 amperes is reached which is held constant for 12 minutes. As the niobium reacts with the carbon from the ethylene, the resistance of the wire increases. Increased voltage is required and temperature of the wire increases from 4200 to 4500°F. At the end of this heating period the C/Nb mole ratio is about 0.55. Extended heating at this temperature will increase the ratio very little. Therefore, the current is increased to 45 amperes for a second 12-minute period at 4900 to 5000°F. The resistance changes little during this period as the C/Nb ratio increases to about 0.8. The composition is equalized by heating in a hydrogen atmosphere for 5 minutes at 4900°F.

F. Preparation of Pyrolytic Graphite Test Specimens

Hemispherical specimens of pyrolytic graphite are being produced for evaluation in plasma torch experiments. These specimens are prepared by the deposition of pyrolytic graphite from methane on an AGOT graphite substrate in an arc image furnace. The furnace consists essentially of two 60-inch General Electric search lights, Model 1942A. One unit generates radiation by a carbon arc and the other collects and focuses. The specimen which is placed at the focal point of the collection mirror can be heated to temperatures as high as 4000°F. The substrate is a 0.5-inch diameter hemisphere of AGOT graphite placed in a cylindrical quartz shroud, 1.5 inches in diameter and six inches in length. The shroud is open at one end and closed at the other except for a tubular gas inlet, 0.5 inches in diameter, which extends into the shroud to a point 3 inches from the specimen. A typical run consists of a short purge of the shroud with nitrogen, introduction of reactant gases into the shroud, and arc initiation. The reactant gases consist of methane at a feed rate of 2.12 SCFH and nitrogen at a feed rate of 30 SCFH. The temperature is held constant at 3600°F, and the production run time is 32 minutes. A typical run results in a 25-mil coating at the stagnation point and an 11-mil coating at the base.

III. FUTURE WORK

Work is now commencing with corrosive gases, HF, HCL and BF_3, in the plasma torch, vacuum reactor, and high-pressure bomb. AGOT graphite will be evaluated in the presence of these gases in plasma torch tests and TaC will be evaluated in the reactor and bomb tests. Additional tests are also planned with ZT and pyrolytic graphites.

INITIAL DISTRIBUTION FOR BU WEPS REACTIONS QPR

Commanding General
Aberdeen Proving Ground
Maryland (1)

Aerojet-General Corporation
P. O. Box 1947
Sacramento, California
Attn: Dr. W. O. Wetmore (2)

Commander
Air Force Ballistic Missile Division
Hq. Air Res. & D v. Command
P. O. Box 262
Inglewood, California
ATTN: WDSOT (1)

Commanding General
U. S. Army Ordnance Missile Command
Redstone Arsenal, Alabama
Attn: Technical Library (2)

Allegany Ballistics Laboratory
Hercules Powder Company
Cumberland, Maryland
Attn: Mr. R. Winer (1)

Army Material Command
Detachment 1
Washington, D. C.
Attn: AMCOR-TB

Commander
Armed Services Technical
Information Agency
Arlington Hall Station
Arlington 12, Virginia
Attn: TIPCR (10)

Defense Metals Information Center
Battelle Memorial Institute
505 King Avenue
Columbus 1, Ohio (1)

Carborundum Company
Research and Development Division
Niagara Falls, New York
Attn: Mr. Bruno Miccioli

Clevite Research Center
Clevite Corporation
Cleveland, Ohio (1)

Jet Propulsion Laboratory
4800 Oak Grove Drive
Pasadena 3, California
Attn: Mr. E. I. Newland
Chief, Reports Group (1)

National Aeronautics & Space Adm.
1512 H Street N. W.
Washington 25, D. C.
Attn: Chief, Division of Research
Information (2)

Commander
U. S. Naval Ordnance Laboratory
White Oak, Silver Springs, Maryland
Attn: Library (1)

Commander Officer
U. S. Naval Propellant Plant
Indian Head, Maryland
Attn: Res. & D v. Department

Director
U. S. Naval Research Laboratory
Washington 25, D. C.
Attn: Mr. J. A. Kies, Code
6210 (1)

Department of the Navy
Bureau of Naval Weapons
Washington 25, D. C.
Attn: RRMA (1)
RMMP (3)
DLI-3 (2)

Commanding Officer
Picatinny Arsenal
Dover, New Jersey
Attn: Library (1)

Solid Propellant Information
Center
Applied Physics Laboratory
Johns Hopkins University
8645 Georgia Avenue
Silver Springs, Maryland (3)

Director, Department of the Navy
Special Projects Office
Washington 25, D. C.
Attn: SP-271 (2)

Commanding Officer
Watertown Arsenal
Watertown 72, Massachusetts
Attn: Tech. Info. Section (1)

Commander
Aeronautical Systems Division
Materials Central
Wright-Patterson Air Force Base
Ohio
Attn: ASRCEE-1 (1)

Commander
Aeronautical Systems Division
Wright-Patterson Air Force Base
Ohio
Attn: ASRCNP (1)

Headquarters, Space Systems Division
Air Force Systems Command
P. O. Box 262, Air Force Unit, P.O.
Los Angeles 45, California
Attn: TDC (1)

Commander
U. S. Naval Ordnance Laboratory
White Oak, Silver Springs 19, Maryland
Attn: Code WM (1)

Commander
U. S. Naval Ordnance Test Station
China Lake, California
Attn: Technical Library Branch (3)

Reaction Motors Division
Thiokol Chemical Corporation
Denville, New Jersey
Attn: Librarian

National Aeronautics & Space Adm.
Lewis Research Center
21000 Brookpark Road
Cleveland 35, Ohio
Attn: Library

National Aeronautics &
Space Administration
George C. Marshall Space
Flight Center
Huntsville, Alabama
Attn: Librarian

Rocket Research Laboratories
Air Force Systems Command
Edwards Air Force Base, Calif.
Attn: DGS (1)

Dept. of Defense
Advanced Research Projects
Agency
Washington 25, D. C.
Attn: Dr. Gene V. Mock (1)

Aeronutronic, A Division of
Ford Motor Company
Ford Road, Newport Beach,
California
Attn: Mr. L. H. Linder
Division Librarian (1)

Applied Physics Laboratory
Johns Hopkins University
8621 Georgia Avenue
Silver Springs, Maryland
Attn: Mr. Paul Drury (1)

Commander
Wright Air Development
Division
Wright-Patterson Air Force
Base
Ohio
Attn: RRLC (1)
WWRCNP (1)
WWRCNC-2 (1)
WWRCMC (Capt. R. H.
Wilson for Nat'l
Carbon Co.) (2)

Union Carbide Corporation
Research Institute
P. O. Box 278
Tarreytown, New York